ISSN 1674-1056
http://cpb.iphy.ac.cn
http://iopscience.iop.org/cpb
中国物理 B
Chinese Physics
中国物理 Chinese Physics B

Investigation of europium(III)-doped ZnS for immunoassay

Chao-Fan Zhu(朱超凡), Xue Sha(沙雪), Xue-Ying Chu(楚学影), Jin-Hua Li(李金华), Ming-Ze Xu(徐铭泽), Fang-Jun Jin(金芳军), Zhi-Kun Xu(徐志堃)
Citation: Chin. Phys. B . 2018, 27(2): 027803. **doi:** 10.1088/1674-1056/27/2/027803

Journal homepage: http://cpb.iphy.ac.cn; http://iopscience.iop.org/cpb

What follows is a list of articles you may be interested in

Electronic structure and photoluminescence property of a novel white emission phosphor $Na_3MgZr(PO_4)_3:Dy^{3+}$ for warm white light emitting diodes

Ge Zhu(朱革), Zhuo-Wei Li(李卓为), Chuang Wang(王闯), Fa-Guang Zhou(周发光), Yan Wen(温艳), Shuang-Yu Xin(辛双宇)
Chin. Phys. B . 2017, 26(9): 097801. **doi:** 10.1088/1674-1056/26/9/097801

Tunable band gap and optical properties of surface functionalized Sc_2C monolayer

Shun Wang(王顺), Yu-Lei Du(杜宇雷), Wen-He Liao(廖文和)
Chin. Phys. B . 2017, 26(1): 017806. **doi:** 10.1088/1674-1056/26/1/017806

Optoelectronic and thermoelectric properties of Zintl YLi_3X_2(X=Sb, Bi) compounds through modified Becke—Johnson potential

T Seddik, G Uğur, R Khenata, Ş Uğur, F Soyalp, G Murtaza, D P Rai, A Bouhemadou, S Bin Omran
Chin. Phys. B . 2016, 25(10): 107801. **doi:** 10.1088/1674-1056/25/10/107801

First-principles studies of electronic, optical, and mechanical properties of γ-$Bi_2Sn_2O_7$

Chao-Hao Hu(胡朝浩), Xue-Hui Yin(殷学辉), Dian-Hui Wang(王殿辉), Yan Zhong(钟燕), Huai-Ying Zhou(周怀营), Guang-Hui Rao(饶光辉)
Chin. Phys. B . 2016, 25(6): 067801. **doi:** 10.1088/1674-1056/25/6/067801

Optical properties of F-and H-terminated armchair silicon nanoribbons

Lu Dao-Bang, Pu Chun-Ying, Song Yu-Ling, Pan Qun-Na, Zhou Da-Wei, Xu Hai-Ru
Chin. Phys. B . 2015, 24(12): 127802. **doi:** 10.1088/1674-1056/24/12/127802

Investigation of europium(III)-doped ZnS for immunoassay*

Chao-Fan Zhu(朱超凡)[1], Xue Sha(沙雪)[1], Xue-Ying Chu(楚学影)[1,†], Jin-Hua Li(李金华)[1], Ming-Ze Xu(徐铭泽)[1], Fang-Jun Jin(金芳军)[1], and Zhi-Kun Xu(徐志堃)[2]

[1] *School of Science, International Joint Research Center for Nanophotonics and Biophotonics, Changchun University of Science and Technology, 7089 Wei-Xing Road, Changchun 130022, China*

[2] *Key Laboratory for Photonic and Electric Bandgap Materials, Ministry of Education, Harbin Normal University, Harbin 150025, China*

(Received 20 July 2017; revised manuscript received 18 October 2017; published online 5 January 2018)

Biofunctional europium (III)-doped ZnS (ZnS:Eu) nanocrystals are prepared by a sol–gel method. The characteristic luminescence of ZnS:Eu is used as a probe signal to realize sensitive immunoassay. The luminescence intensity of the Eu^{3+} in the ZnS matrix shows strong concentration dependence, and the optimal doping concentration is 4%. However, the emission wavelengths of the ZnS:Eu nanocrystals are not dependent on doping concentration nor the temperature (from 100 K to 300 K). Our results show that these features allow for reliable immunoassay. Human immunoglobulin, used as a target analyte, is captured by antibody modified ZnS:Eu probe and is finally enriched on gold substrate for detection. High specificity of the assay is demonstrated by control experiments. The linear detection range is 10 nM–800 nM, and the detection limit is about 9.6 nM.

Keywords: ZnS:Eu, optical properties, immunoassay

PACS: 78.55.–m, 68.35.bg, 78.55.Et **DOI:** 10.1088/1674-1056/27/2/027803

1. Introduction

The rapid development of nanotechnology and biomedicine has greatly aroused interest in the research of semiconductor nanomaterials for biomedical applications.[1] CdSe quantum dots and their core shell structures are the most active luminescent materials currently used in the study of biological markers.[2] However, the toxicity of heavy metal ions has received much attention of researchers and restricts its applications in the fields of biology, medicine, pharmacy, etc.[3,4] Therefore, the development of a new non-toxic matrix material as a fluorescent marker is necessary. The ZnS nanomaterials are non-toxic and exhibit good biological compatibility and chemical stability in the physiological environment, even in a high salt alkali environment.[5] The ZnS nanomaterials can be activated by appropriate element doping, which can greatly improve their luminous performance.[6]

Rare-earth ions are an attractive candidate for doping due to the unique optical properties originating from their special features of electronic configurations.[7] Eu^{3+} ion, as a typical member of rare-earth ions, is one of the most important activators in red luminescent materials.[8] The Eu^{3+}-activated luminescent materials are widely used in fluorescent lamps, cathode ray tubes, and plasma display panels.[9] However, immunoassay based on the fluorescence spectrum of Eu^{3+} is nearly ignored. Recently, ultrasensitive immunoassay based on CdS:Eu nanoparticles was reported by Liu *et al.*[10] The strategy is based on the quenching of the electrochemiluminescence from CdS:Eu. In fact, the fluorescence spectrum of Eu^{3+} is comprised of several narrow and intense emission lines, which can be used as a characteristic signal to carry immune detection.[11] Since the nontoxicity and easy doping of ZnS, Eu^{3+}-doped nanomaterial with using ZnS as the matrix will be conducive to the obtaining of an environmental friendly fluorescent immune detection.[12]

Herein, ZnS:Eu nanomaterials are prepared by a sol–gel method and biofunctionalized by introducing carboxyl groups. The optical property of the ZnS:Eu nanomaterials is optimized by doping concentration. The wavelength positions of the emission lines are anti-interference by temperature, which provides an accurate and reliable detection. The detection results show that rare-earth-doped ZnS nanomaterials can be used in immunoassays.

2. Experimental section

2.1. Chemicals and materials

The $Zn(AC)_2{\cdot}2H_2O$ and $Na_2S{\cdot}9H_2O$ were obtained from Sigma–Aldrich. Thioctic acid (TA), 3-Mercaptopropionic acid (MPA), N-Hydroxysulfosuccinimide sodium salt (NHSS), and $Eu(NO)_3{\cdot}6H_2O$ were purchased from Aladdin Reagent Company Limited (Co., LTD). 1-ethyl-3-[3-dimethylaminopropyl] carbodiimide (EDC), Bovine serum albumin (BSA), goat anti-human immunoglobulin (IgG) and human IgG were purchased from Beijing Dingguo biotechnology Co., LTD. All chemicals were of analytical grade in purity and directly used without

*Project supported by the National Natural Science Foundation of China (Grant No. 61205193), the Project of Science and Technology of Jilin Province, China (Grant No. 20140520107JH), the Technology Foundation of Jilin Provincial Department of Human Resources and Social Security, China (Grant No. RL201306), and the Science Foundation for Young Scientists of Changchun University of Science and Technology, China (Grant No. XQNJJ-2015-03).

†Corresponding author. E-mail: chuxy608@163.com

© 2018 Chinese Physical Society and IOP Publishing Ltd

being purified further.

2.2. Preparation of the biofunctional ZnS:Eu nanomaterials

Aqueous synthesis not only solves the problem of the water solubility of the nanomaterials, but also is simpler, less toxic and less expensive than the metal–organic chemical method. Thus, ZnS:Eu nanomaterials were prepared by a modified aqueous method.[13] The improvement was that the carboxyl groups were introduced by MPA to gain a biofunctional surface. The detailed process is as follows: 300-μl MPA was added into 50-ml 75-mM $Zn(AC)_2{\cdot}2H_2O$ aqueous solution; 50-ml 0.75-mM $Eu(NO)_3{\cdot}6H_2O$ was added in the mixing process for the 1% doped ZnS:Eu sample. After mixing for 20 min, 50-ml 75-mM $Na_2S{\cdot}9H_2O$ solution was slowly added to the mixed solution to provide element sulphur. Stirring continued for 3 h to obtain ZnS:Eu sample. The concentration of the Eu^{3+} was amplified to prepare 2% (3%, 4%, and 5%) doped samples.

2.3. Preparation of ZnS:Eu-antibody fluorescent probes

The principle for preparing the fluorescent probe and the sandwich immunoassay is depicted in Fig. 1. For preparing the probe, the as-prepared ZnS:Eu nanomaterial solution (2 ml) was dispersed in deionized water (0.5 ml) after centrifugation. An EDC/NHSS aqueous solution (0.1 M/0.02 M) was mixed with the ZnS:Eu solution and was rocked for 15 min, to assist the coupling of the antibody.[14] Then, 660-nM goat anti-human IgG was added and rocked at 37 °C for 1 hour. The 1.5-ml BSA solution with a mass concentration of 1% was used to block the remaining bind sites to avoid nonspecific absorption. Finally, the obtained probe was dispersed in aqueous solution (1.5 ml) after being centrifuged.

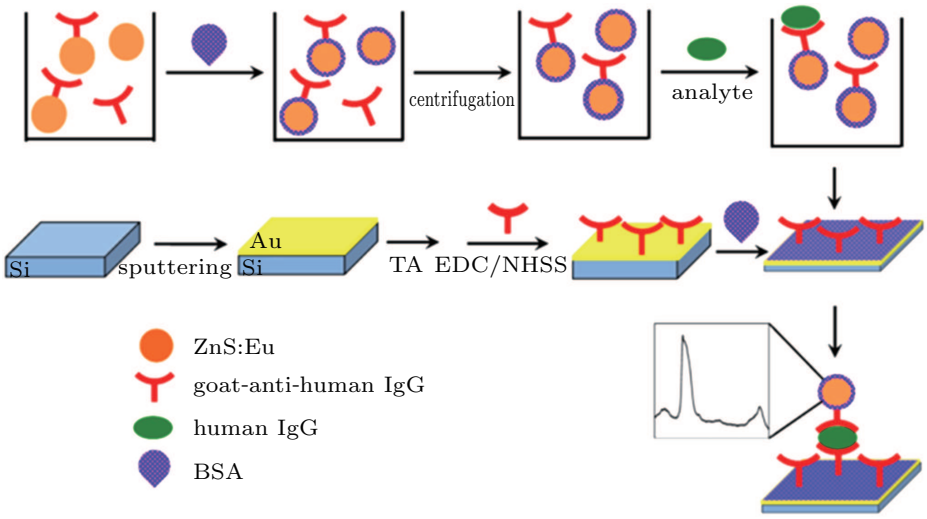


Fig. 1. (color online) Schematic diagram of the ZnS:Eu based immunoassay.

2.4. Immune assembly of Au substrate

The Au substrate assembly we used in the present investigation (for details, see the research work of Meyerhoff *et al.*)[15] was obtained by depositing a layer of Au on a single-crystal silicon in vacuum. Because Au and other sulfur containing groups are prone to coordination processes,[16] carboxyl groups were introduced by immersing the Au substrate in a 2% ethanol solution of TA for 24 hours. In each of the following steps, the substrates were carefully rinsed and then dried by using a nitrogen flow. The substrate was then immersed in an EDC/NHSS aqueous solution for 45 min to activate carboxylate groups, followed by a goat anti-human IgG (660 nM) solution at 37 °C with continual rocking for 2 hours. The BSA aqueous solution (1 wt%) was also introduced to avoid nonspecific absorption by incubation for 2 hours at 37 °C. Finally, the Au substrate with immobilized antibody was prepared.

2.5. Immune detection based on ZnS:Eu nanomaterials

Control experiments were performed to verify the immune function of the nanomaterials. First, the gold substrate was directly immersed into the prepared ZnS:Eu probe solution for 2 h as the blank test. Second, a specified concentration of human IgG molecules (1 μM) was added to the probe solution and rocked for 2 h for analyte capturing. After being centrifuged and redispersed, the solution containing the probes/analyte complexes was prepared. The Au substrate with immobilized antibody was immersed in the solution for 2 h at 37 °C with gentle shaking. Then, the substrate was carefully rinsed and then dried using a nitrogen flow. To verify the sensitivity, five control experiments were performed. The 800 nM (or 600 nM, 400 nM, 200 nM, 100 nM, 10 nM) human IgG was added to the probe solution with all other experimental conditions being the same as those in the second experiment. An unspecific control experiment was also carried out to evaluate the selectivity, where the analyte (human

IgG) was replaced with 1-μM rabbit IgG.

2.6. Characterization

Transmission electron microscopy (TEM) images were obtained on a JEOL JEM-2200FS microscope operated at 200 kV. Selected area electronic diffraction (SAED) attached to the TEM was used to analyze the crystal structure. The structure was further determined by x-ray diffraction (XRD, Rigaku D/max 2500). The existence of Eu element and the bonding state were confirmed by x-ray photoelectron spectroscopy (XPS, VG ESCALAB LKII) with a binding energy reference of 284.6 eV for a C 1s line. Fluorescence investigations were performed on the samples by using a Shimadzu RF-5301PC fluorescence (FL) spectrometer with an excitation wavelength of 396 nm. Photoluminescence (PL) investigations of the sample were carried out with a Horiba LabRam HR evolution spectrophotometer excited with a 532-nm laser. For temperature-dependent photoluminescence, the temperature variation range is from 300 K to 100 K.

3. Results and discussion

3.1. Morphology and crystal structure

The morphology and the structure of the synthesized sample are investigated by TEM and SAED measurements. Figure 2(a) shows the high resolution TEM (HRTEM) image of the formed ZnS:Eu nanoparticles with a doping concentration of 4%. The inset in Fig. 2(a) shows a large field TEM image. Clear lattice fringes of the sample are observed. The crystal structure of the ZnS:Eu nanoparticles is determined by using an SAED as shown in Fig. 2(b).

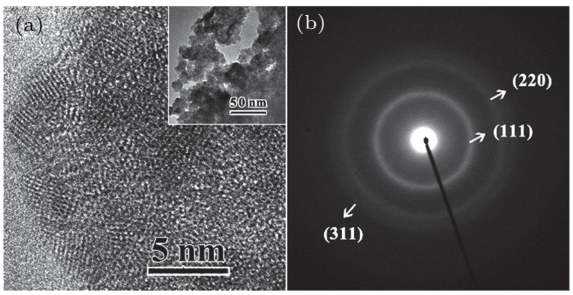


Fig. 2. (a) HRTEM image, with inset showing TEM image of a larger area, and (b) SAED pattern.

The interplanar distances calculated by using the three diffraction rings are 3.10 Å, 1.90 Å, and 1.57 Å, which coincide with those of the (111), (220), and (311) planes of cubic zinc-blende ZnS, respectively. The results of XRD measurement further confirms the crystal structure (Fig. 3). No other diffraction peaks are observed, indicating no obvious impurities. The positions of the (111) peaks of undoped ZnS and ZnS:Eu (1%–4%) nanocrystals are located at 28.77°, 28.56°, 28.44°, 28.23°, 28.03°, respectively. When Zn^{2+} is replaced by Eu^{3+}, lattice expansion of ZnS can be caused, which leads to the shift toward the lower degree direction.[17] The XPS measurement is performed to confirm the existence of Eu element and the bonding states in ZnS:Eu nanomaterials. As shown in Fig. 4, the characteristic peak at 1135.7 eV is attributed to the core level of Eu 3d 5/2, which indicates that the Eu ions are trivalent.[18]

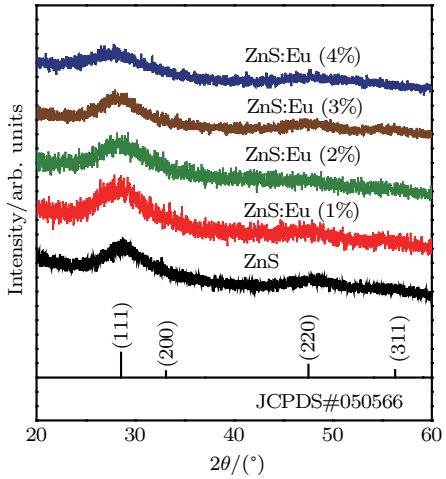


Fig. 3. (color online) XRD pattern of the ZnS:Eu nanomaterials with different doping concentrations.

3.2. Fluorescence properties

The influence of Eu^{3+} doping concentration on the luminescence intensity is discussed in this paper. Figure 5 shows the emission spectra of samples all diluted to the same extent with an excitation wavelength of 396 nm. The doping concentration is varied from 1% to 5%. Three emission peaks located at 594 nm, 617 nm, and 714 nm are clearly observed. The weak emission peak, which is located at 594 nm, comes from the emission of the $^5D_0 \rightarrow {}^7F_1$ transition in Eu^{3+}. The strong emission peak at 617 nm is attributed to the $^5D_0 \rightarrow {}^7F_2$ transition, and the other emission around 714 nm arises from the $^5D_0 \rightarrow {}^7F_4$ transition.[19] The intensity ratio between transitions of $^5D_0 \rightarrow {}^7F_2$ and $^5D_0 \rightarrow {}^7F_1$ is called the asymmetry ratio, and is used to effectively detect the symmetry of the Eu^{3+} ion crystal lattice through using the spectrum.[20] The luminescence intensity of the electric dipole transition at 617 nm ($^5D_0 \rightarrow {}^7F_2$) is higher than that of the magnetic dipole transition located in 594 nm ($^5D_0 \rightarrow {}^7F_1$), which can be explained by Eu^{3+} occupying the lattice position off the inversion center.[21] The increasing of the doping concentration gradually increases the intensity of emission peak, until it reaches up to 4%. When the doping concentration increases to 5%, the fluorescence intensity decreases due to the concentration quenching effect.[22] The inset of Fig. 5 shows the relationship between the fluorescence intensity and the doping concentration. Whereas the doping concentration has no influence on the peak wavelength of the emission, indicating that the ZnS:Eu sample with any doping concentration possesses characteristic fluorescence which can provide uniform detection result in the following immunoassays.

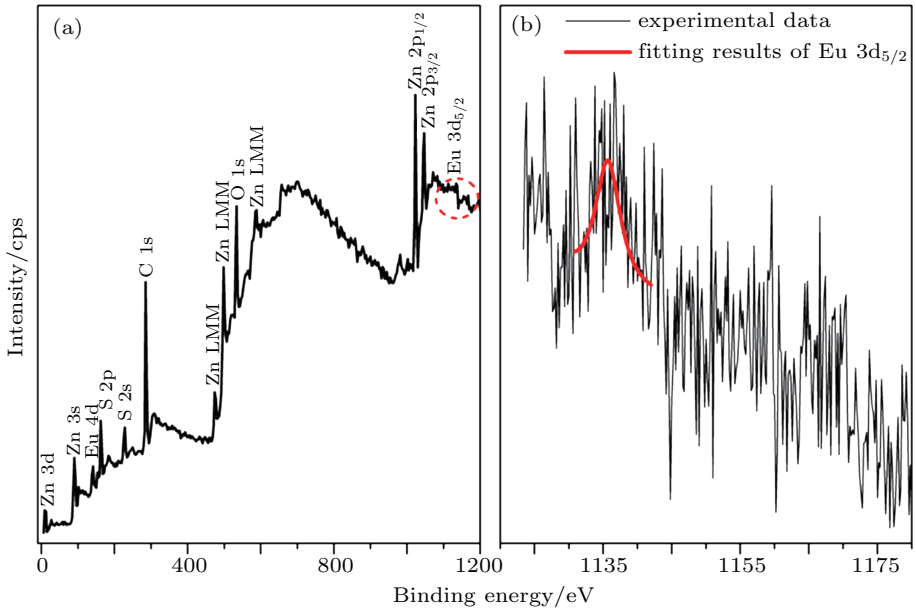


Fig. 4. (color online) XPS spectrum of ZnS:Eu (4%): (a) XPS survey spectrum; (b) Eu 3d XPS spectrum.

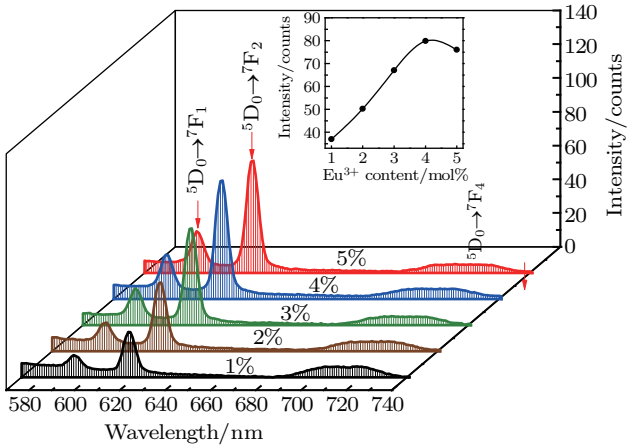


Fig. 5. (color online) Fluorescence emission spectra of liquid samples containing ZnS:Eu nanomaterials with different doping concentrations. The inset shows the relationship between the fluorescence intensity and the doping concentration.

Except for the doping concentration, the influence of temperature on the fluorescence is also investigated. Considering the fact that biomolecular may lose activities under high temperature, the temperature range in PL measurement is from 300 K to 100 K. A 532-nm laser is chosen as the excited light to obtain more detailed information about the emissions from Eu^{3+} ion.[23] With respect to the fluorescence excited by a xenon lamp (as shown in Fig. 5), more $^5D_0 \rightarrow {}^7F_J$ ($J = 0$, 1, 2, 3, 4) transitions can be observed (see Fig. 6). It is obvious that there is a series of emission sites in Fig. 6, which are the characteristic emissions of Eu^{3+} ion,[18] corresponding to the $^5D_0 \rightarrow {}^7F_0$, $^5D_0 \rightarrow {}^7F_1$, $^5D_0 \rightarrow {}^7F_2$, $^5D_0 \rightarrow {}^7F_3$, $^5D_0 \rightarrow {}^7F_4$ transitions, respectively. As the temperature decreases, the intensity of light emission gradually decreases, which may result from the surface effect and the local environment changes of Eu^{3+} in the surface layers.[24] However, the peak positions of the luminescence do not change, indicating that the wavelength of the fluorescence is independent of temperature. This will be essential to the distinguishing of the origin of the signal in photoluminescence measurements (the signal is derived from the background or the biolabels), especially for ultralow concentration detections.

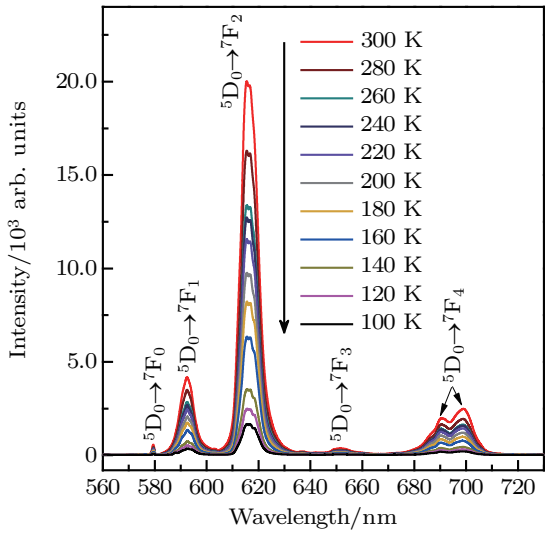


Fig. 6. (color online) Photoluminescence spectra of ZnS:Eu varying with temperature for an excitation wavelength of 532 nm.

3.3. Immunoassays based on the ZnS:Eu probes

The principle used for this assay is similar to a sandwiched enzyme-linked immunosorbent assay (ELISA). Compared with the ELISA, the step of adding an enzymatic substrate is omitted, and the enzyme is replaced by ZnS:Eu nanocrystal, which can provide simpler and more robust as-

says. The 4% doped ZnS:Eu nanomaterial presents the optimal fluorescence and is chosen as the biolabel to perform immunoassays. A 532-nm laser is used as an excitation source. Figure 7 shows the immune detection results. For sandwiched structures with 1-μM analyte, the characteristic emissions of Eu^{3+} at 714 nm, 617 nm, 594 nm, and 580 nm can be observed. For immune detections, blank and unspecific group experiments can avoid the false positive signal. No analyte is added in the blank control group, and human IgG is replaced by 1-μM rabbit IgG in the unspecific group. The luminescence signal of the ZnS:Eu is observed in neither of the control groups (see Fig. 7), indicating good specificity of the immunoassay. To evaluate the performance of the current assay, the concentration of the analyte decreases from 800 nM to 10 nM. Statistical analysis based on repeated immunoassay indicates that the intensity of the fluorescence gradually decreases with analyte concentration decreasing [Fig. 7(b)]. The regression curve equation is "$Y = 17.2226 + 0.0584X$", and correlation coefficient is 0.9921. The linear range is 10 nM–800 nM. The detection limit is worked out by the "$3\sigma/S$", where S is the slope of the curve equation, and σ represents the standard deviation for the blank sample. The calculated detection limit is 9.6 nM. The sensitivity of the current stage ZnS:Eu based assay is similar to that of commercially available ELISA, and the promising prospects can be expected due to the advantages of the current assay.

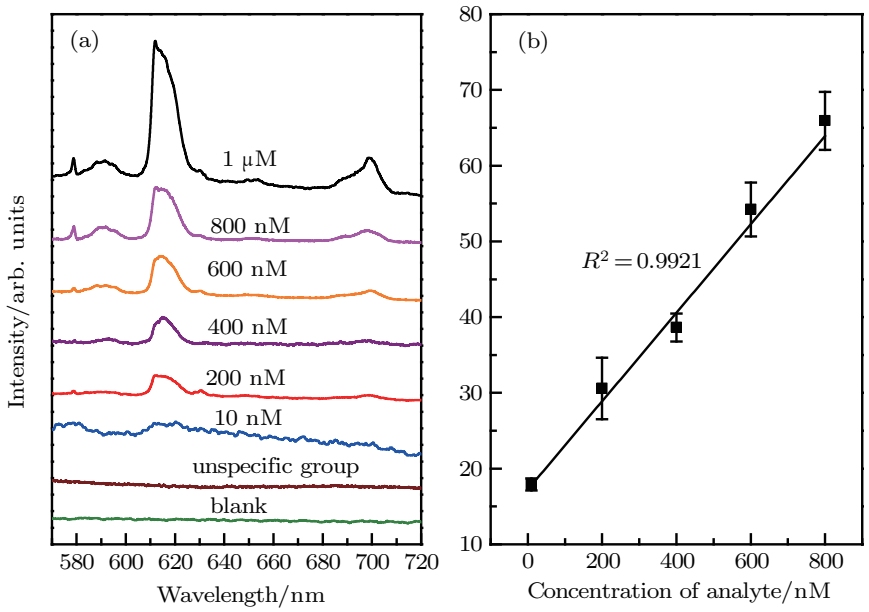


Fig. 7. (color online) (a) Photoluminescence spectra of the sandwich structures with different concentrations of the analyte. (b) Plot of photoluminescence intensity at 617 nm versus analyte concentration, with error bars indicating standard deviation.

4. Conclusions and perspectives

An immunoassay is performed by using biofunctionalized ZnS:Eu semiconductor nanocrystals as fluorescent probes. The optimal doping concentration to obtain ZnS:Eu nanomaterials with high fluorescent emission is 4%. The further increasing of the doping concentration will lead to fluorescence quenching. The photoluminescence peak position of the emission originating from $^5D_0 \rightarrow {}^7F_2$ transition is always around 617 nm when the temperature varies from 100 K to 300 K, which allows the accurate determination of human IgG. The fluorescent probes show high specificity for the target analyte, and the calculated detection limit is about 9.6 nM. The strategy of using Eu^{3+} doped zinc-based semiconductor can be extended to other materials, such as ZnO, and may play an important role in future biomedicine.

References

[1] Taylor-Pashow K M L, Rocca J D, Huxford R C and Lin W B 2010 *Chem. Commun.* **46** 5832
[2] Silva A C, Freschi A P, Rodrigues C M, Matias B F, Maia L P, Goulart L R and Dantas N O 2016 *Nanomedicine* **12** 1421
[3] Wang L, Fu J, Chen H Q, Liang A, Qian B B, Ling B and Zhou C L 2010 *J. Lumin.* **130** 845
[4] Béchard K M, Gillis P L and Wood C M 2008 *Arch. Environ. Con. Tox* **54** 454
[5] Ding Y D, Cong T, Chu X Y, Jia Y, Hong X and Liu Y C 2016 *Anal. Bioa. Chem.* **408** 5013
[6] Xie H Q, Chen Y, Huang W Q, Huang G F, Peng P, Peng L, Wang T H and Zeng Y 2011 *Chin. Phys. Lett.* **28** 027806
[7] Mai H X, Zhang Y W, Si R, Yan Z G, Sun L D, You L P and Yan C H 2006 *J. Am. Chem. Soc.* **128** 6426
[8] Chen X L, Chen X Y, Wei X D, Cai L Y, Lu F C and Liu Q L 2009 *Chin. Phys. B* **18** 3555
[9] Sadhu S, Chowdhury P S and Patra A 2008 *J. Lumin.* **128** 1235
[10] Liu J, Cui M R, Zhou H and Zhang S S 2016 *Sci. Rep.* **6** 30577
[11] Liu S M, Guo H Q, Zhang Z H, Liu F Q and Wang Z G 2000 *Chin. Phys. Lett.* **17** 609

[12] Ashwini K, Pandurangappa C and Nagabhushana B M 2012 *Phys. Scr.* **85** 065706
[13] Lotey G S, Jindal Z, Singhi V and Verma N K 2013 *Mater. Sci. Semicond. Process.* **16** 204450
[14] Das M, Mishra D, Maiti T K, Basak A and Pramanik P 2008 *Nanotechnology* **19** 415101
[15] Duan C and Meyerhoff M E 1995 *Microchim. Acta* **117** 195206
[16] Ulman A 1996 *Chem. Rev.* **96** 1533
[17] Ahemen I, Amah A N, AttahDaniel B E and Fasasi A Y 2014 *Nanosci. Nanotechnol.* **4** 7
[18] Poornaprakash B, Poojitha P T, Chalapathi U and Park S 2016 *Mater. Lett.* **181** 227
[19] Sun L D, Yan C H, Liu C H, Liao C S, Li D and Yu J Q 1998 *J. Alloys Compd.* **275–277** 234
[20] Fujihara S, Kojia S and Kimura T 2004 *J. Mater. Chem.* **14** 1331
[21] Aneesh P M and Jayaraj M K 2010 *Bull. Mater. Sci.* **33** 227
[22] Bang H, Morishima S, Sawahata J, Seo J, Takiguchi M, Tsunemi M, Akimoto K and Nomura M 2004 *Appl. Phys. Lett.* **85** 227
[23] Kassab L R P, Silva D S D, Almeida R D, and Araújo C B D 2009 *Appl. Phys. Lett.* **94** 101912
[24] Wang D Y, Wang Q K, Chang Z Y, Guo Y Y and Wu X H 2009 *J. Inorg. Mater.* **24** 239